

## Effect of TiO<sub>2</sub> on the crystallization behaviors and microstructure of glazes based on MgO-Al<sub>2</sub>O<sub>3</sub>-SiO<sub>2</sub> system

Yoorim Rho<sup>a</sup>, Kangduk Kim<sup>a,\*</sup> and Jin-Ho Kim<sup>b,\*\*</sup>

<sup>a</sup>Department of Advanced Materials Engineering, Kyonggi University, Suwon 16227, Korea

<sup>b</sup>Ceramic Ware Center, Korea Institute of Ceramic Engineering & Technology, Icheon 17303, Korea

A MgO-Al<sub>2</sub>O<sub>3</sub>-SiO<sub>2</sub> system was used in order to prepare glass-ceramic glazes with high-hardness applicable to ceramic tiles. The glass-ceramic glazes were prepared by adding the fluxes CaO and B<sub>2</sub>O<sub>3</sub> and the nucleating agent TiO<sub>2</sub> to the glaze. The crystallization behavior of the glaze was calculated by a non-isothermal thermal analysis via a Differential Thermal Analysis (DTA), and the glaze was heat treated at the crystallization temperature (T<sub>p2</sub>). The activation energy (E) and the Avrami constant (n) of the glaze with 8wt% TiO<sub>2</sub> substitution were 177.07 kJ/mol and 2.65, respectively. X-ray diffraction analysis (XRD) showed that the cordierite and anorthite crystal phases were formed and the karrooite crystal phases grew with increasing TiO<sub>2</sub> substitution. The degree of crystallinity increased as the amount of TiO<sub>2</sub> increased and the degree of crystallinity was 76.5% in the glaze with 8 wt% TiO<sub>2</sub> substitution. In the Scanning Electron Microscope (SEM) analysis, the cordierite and anorthite crystal phases were the largest in the glaze with 8wt% TiO<sub>2</sub> substitution and rapidly decreased in the glaze with 12 wt% TiO<sub>2</sub> substitution. As a result, Vickers hardness of the glaze showed a high value of 7.10 GPa at the glaze with 8wt% TiO<sub>2</sub> substitution after heat treatment at 1,010 °C.

**Keywords:** Glass-Ceramic Glaze, Cordierite, TiO<sub>2</sub> nucleation agent, Hardness, Avrami constant.

### Introduction

Glaze used as a coating film on the surface of porcelain and ceramic tiles protects the ceramic body from external contamination, provides physical properties such as strength and hardness, and contributes to the high value of ceramic products [1]. The friction and the wear characteristics of the conventional amorphous glaze are not sufficient, however, and various studies have been conducted on the development of a glaze having high wear resistance and hardness, excellent chemical resistance, and low porosity [2]. Recently, studies have been actively conducted to improve the characteristics of the glaze through a glass-ceramic glaze that crystallizes its amorphous structure. Glass-ceramic glazes have been reported to exhibit various physical/chemical properties, depending on the type of crystalline phase and degree of crystallinity [3]. Furthermore, studies have been conducted on glass-ceramic glazes which to improved mechanical properties through micro/nanostructured control and to reduce cost by using industrial residues as a raw materials [4-6].

Glass-ceramic glazes are prepared by melting and quenching the amorphous frit and then inducing nucleation

and growth at the crystallization temperature [7]. Some amorphous frit itself is self-nucleating, but nucleation and phase separation is promoted in most amorphous frit by the addition of nucleating agents [8]. As a general nucleating agent, TiO<sub>2</sub>, Cr<sub>2</sub>O<sub>3</sub>, Fe<sub>2</sub>O<sub>3</sub>, CaF<sub>2</sub>, WO<sub>3</sub>, V<sub>2</sub>O<sub>5</sub> or MoO<sub>3</sub> is used[9]. Zircon-based glass-ceramic glazes are widely used in most glass-ceramic glazes due to their high temperature stability, high refractive index, whiteness, high hardness, and chemical resistance of the zircon (ZrSiO<sub>4</sub>) crystal phase. However, due to the high price, there is a need for research on the composition of low-cost frit to replace zircon [1, 9]. In response, MgO-Al<sub>2</sub>O<sub>3</sub>-SiO<sub>2</sub>, Li<sub>2</sub>O-Al<sub>2</sub>O<sub>3</sub>-SiO<sub>2</sub>, CaO-MgO-SiO<sub>2</sub>, CaO-Al<sub>2</sub>O<sub>3</sub>-SiO<sub>2</sub>, and ZnO-Al<sub>2</sub>O<sub>3</sub>-SiO<sub>2</sub> systems based high strength glass-ceramic glazes have been actively researched[10]. In particular, MgO-Al<sub>2</sub>O<sub>3</sub>-SiO<sub>2</sub> system based glass-ceramic glaze compositions that can form cordierite and mullite crystalline phases having high mechanical strength are attracting attention. Cordierite (2MgO-2Al<sub>2</sub>O<sub>3</sub>-5SiO<sub>2</sub>) crystals have a low coefficient of thermal expansion (~10-22 × 10<sup>-7</sup> °C<sup>-1</sup>; 25-800 °C), low dielectric constant, high chemical durability, high heat resistance, and good mechanical properties [11, 12]. X. J. Hao et al. increased the degree of crystallinity of the glass by changing the heat treatment conditions in the MgO-Al<sub>2</sub>O<sub>3</sub>-SiO<sub>2</sub> system, and produced a hardened cordierite phase crystal glass of 8.4 GPa [13]. J. T. Francisco et al. added the nucleating agent TiO<sub>2</sub> and the flux B<sub>2</sub>O<sub>3</sub> to the CaO-MgO-Al<sub>2</sub>O<sub>3</sub>-SiO<sub>2</sub> system and developed a cordierite glass-ceramic glaze through a

\*Corresponding author:  
Tel: +82-10-6206-6290  
E-mail: solidwaste@kyonggi.ac.kr  
\*\*Co-corresponding author:  
Tel: +82-10-8914-8707  
E-mail: jino.kim@kicet.re.kr

rapid single heat treatment process [14]. G. Sumana et al. reduced the surface roughness to 3.73  $\mu\text{m}$  and increased the Vickers hardness to 5.04 GPa through microwave sintering in a  $\text{CaO-MgO-Al}_2\text{O}_3\text{-SiO}_2$  system [15].

In this study, cordierite based glass-ceramic glaze was prepared by adding  $\text{B}_2\text{O}_3$  and  $\text{CaO}$  as flux and  $\text{TiO}_2$  as a nucleating agent to  $\text{MgO-Al}_2\text{O}_3\text{-SiO}_2$ . The crystallization mechanism of the cordierite based glass-ceramic glaze according to the amount of added  $\text{TiO}_2$  was analyzed, and the production of a glass-ceramic glaze with high hardness was studied through a correlation analysis between the crystalline phase type, degree of crystallinity, and microstructure.

### Experimental Materials and Methods

To prepare the  $\text{MgO-Al}_2\text{O}_3\text{-SiO}_2$  system glass-ceramic glaze with a cordierite crystalline phase,  $\text{MgO}$  (KOJUNDO Chemical Co., 99.9%, Japan),  $\text{Al}_2\text{O}_3$  (SANCHUN PURE Chemical Co., 99.0%, Korea) and  $\text{SiO}_2$  (KOJUNDO Chemical Co., 99.9%, Japan) were used as the main raw materials.  $\text{B}_2\text{O}_3$  (KOJUNDO Chemical Co., 99.9%, Japan) and  $\text{CaCO}_3$  (KOJUNDO Chemical Co., 99%, Japan) were added as flux, and  $\text{TiO}_2$  (KOJUNDO Chemical Co., 99.9%, Japan) was added as a nucleating agent. The batch composition of the glazes is shown in Table 1. The batch compositions were milled and mixed through a dry ball mill for 24 h using zirconia balls. They were then placed in an alumina crucible, melted at 1,450  $^\circ\text{C}$  for 1 h and 30 min in an electric furnace, and then cooled to room temperature in distilled water. The prepared glaze was crushed to 45  $\mu\text{m}$  or less and subjected to a differential thermal analysis (DTA, STA S1500, Scinco Co., Korea) under conditions of a temperature increase rate of 15  $^\circ\text{C}/\text{min}$ . In addition, the DTA analysis was performed by changing the rate of temperature increase to 5, 10, 15, and 20  $^\circ\text{C}/\text{min}$  in each composition. Through this analysis, the change of crystallization temperature ( $T_p$ ) with or without addition of the nucleating agent was observed, and the activation energy ( $E$ ) and Avrami constant ( $n$ ), which are kinetic parameters of crystallization behavior, were calculated. The  $E$  value was calculated using Eq. (1) proposed by Kissinger [16].

$$\ln\left(\frac{a}{T_p^2}\right) = \left(\frac{-E}{RT_p}\right) + \text{const.} \quad (1)$$

**Table 1.** The batch composition of the glazes.

Specimen	Composition (wt%)					
	MgO	$\text{Al}_2\text{O}_3$	$\text{SiO}_2$	$\text{B}_2\text{O}_3$	$\text{CaCO}_3$	$\text{TiO}_2$
0T	12.00	24.00	50.00	6.00	14.28	-
4T	11.52	23.04	48.00	5.76	13.71	4.00
8T	11.04	22.08	46.00	5.52	13.14	8.00
12T	10.56	21.12	44.00	5.28	12.56	12.00

In the above equation,  $\alpha$  is the heating rate,  $T_p$  is the maximum crystal growth temperature,  $E$  is the activation energy, and  $R$  is the gas constant. The value of  $n$  is calculated using Eq. (2), proposed by Augis-Bennett [16].

$$n = \frac{2.5}{\Delta T_{\text{FWHM}}} \times \frac{RT_p^2}{E} \quad (2)$$

In the above equation,  $n$  is the Avrami constant and  $\Delta T_{\text{FWHM}}$  is the full width at half maximum of the  $T_p$  peak. Based on the results of the DTA analysis, the glass-ceramic glazes was prepared by annealing for 1 h at  $T_{p2}$  of each composition under a heating rate of 15  $^\circ\text{C}/\text{min}$  in an electric furnace. Table 2 shows the composition and heat treatment conditions for the preparation of the glass-ceramic glaze.

The crystalline phases of the glass-ceramic glaze were observed by X-ray diffraction analysis (XRD, Pan'alytical, X'pertpro, Netherlands). X-ray diffraction analysis (XRD, D8 ADVANCE, Bruker Co., USA) was used to measure the degree of crystallization of the glaze using the EVA program. The degree of crystallinity was calculated using the formula proposed by Benedetti's below [17].

$$\% \text{ Crystallinity} = \frac{A_c}{A_c - A_a} \times 100 \quad (3)$$

In the above equation,  $A_c$  is the area of crystallinity scattering and  $A_a$  is the area of amorphous scattering. The microstructure of the glass-ceramic glaze was confirmed using Scanning Electron Microscopy (Nova NanoSEM 450, FEI Co., USA), and a qualitative analysis was performed by Energy Dispersive X-ray Spectroscopy (EDS, EMAX 7593H, HORIBA, Ltd., Japan). For the microstructure analysis, the specimen was prepared by polishing the surface of the glaze and etching for 30 seconds with 3 wt% hydrofluoric acid (HF). The density and the water absorption of the glass-ceramic glaze were measured by the experimental method described in KS L 1001. Drying weight was measured at room temperature, and the suspended weight and water content weight were measured after immersion in distilled water for 24 h.

$$\rho = \frac{W_1}{W_2 - W_3} \quad (4)$$

$$\% \text{ Water absorption} = \frac{W_3 - W_1}{W_1} \times 100 \quad (5)$$

**Table 2.** The composition and heat treatment conditions for the preparation of the glass-ceramic glaze.

Specimen I.D	Sintering	
	Temperature ( $^\circ$ )	Hours
0T	1,085	
4T	1,091	
8T	1,010	1
12T	1,028	

In the above equation,  $\rho$  is the density,  $w_1$  is the dry weight,  $w_2$  is the water content weight, and  $w_3$  is the suspended weight. The hardness of the glaze surface was measured by applying a load of 1 kgf using a Vickers hardness tester (HM-124, MITUTOYO Co., Japan).

## Result and Discussion

Fig. 1 shows the results of the DTA analysis of the glaze under a rate of temperature increase of 15 °C/min. Two crystallization peaks ( $T_p$ ) were observed in all glazes:  $T_{p1}$  was observed below 900 °C and  $T_{p2}$  below 1,100 °C. The crystallization peak of the glass-ceramic glass is observed in the form of exothermic peaks in the DTA analysis because it releases energy while changing from an amorphous structure in a disordered arrangement with a high energy state to a crystalline structure in a regular arrangement with a low energy state [18]. Crystallization temperatures of each composition were 875 °C ( $T_{p1}$ ), 1,085 °C ( $T_{p2}$ ) at 0T, 850 °C ( $T_{p1}$ ) at 4T, 1,085 °C ( $T_{p2}$ ), 849 °C ( $T_{p1}$ ) at 8T, 1,010 °C ( $T_{p2}$ ), 12T at 858 °C ( $T_{p1}$ ), and 1,028 °C ( $T_{p2}$ ). The lowest crystallization peak was observed in the composition to which TiO<sub>2</sub> was added 8 wt%.

In order to analyze the crystallization behavior of glazes by composition, a non-isothermal thermal analysis

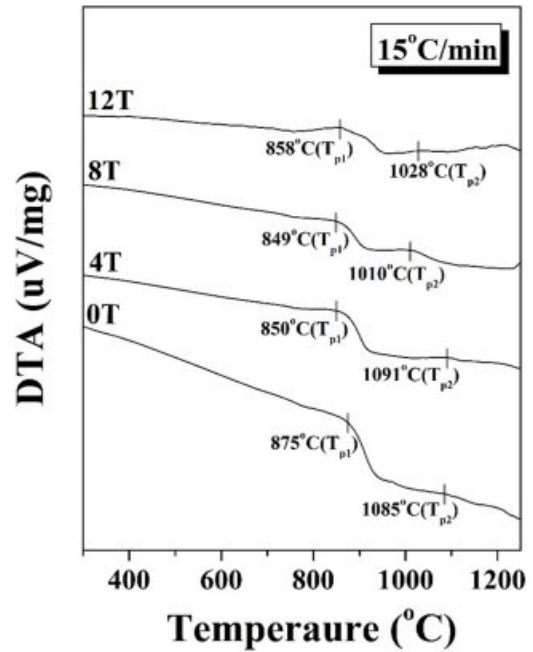


Fig. 1. The DTA analysis of the glaze under a rate of temperature increase of 15 °C/min.

was carried out with change of the heating rate (5, 10, 15, 20 °C/min) with DTA. The activation energy ( $E$ ) calculated by Kissinger's equation (1) is shown in Fig.

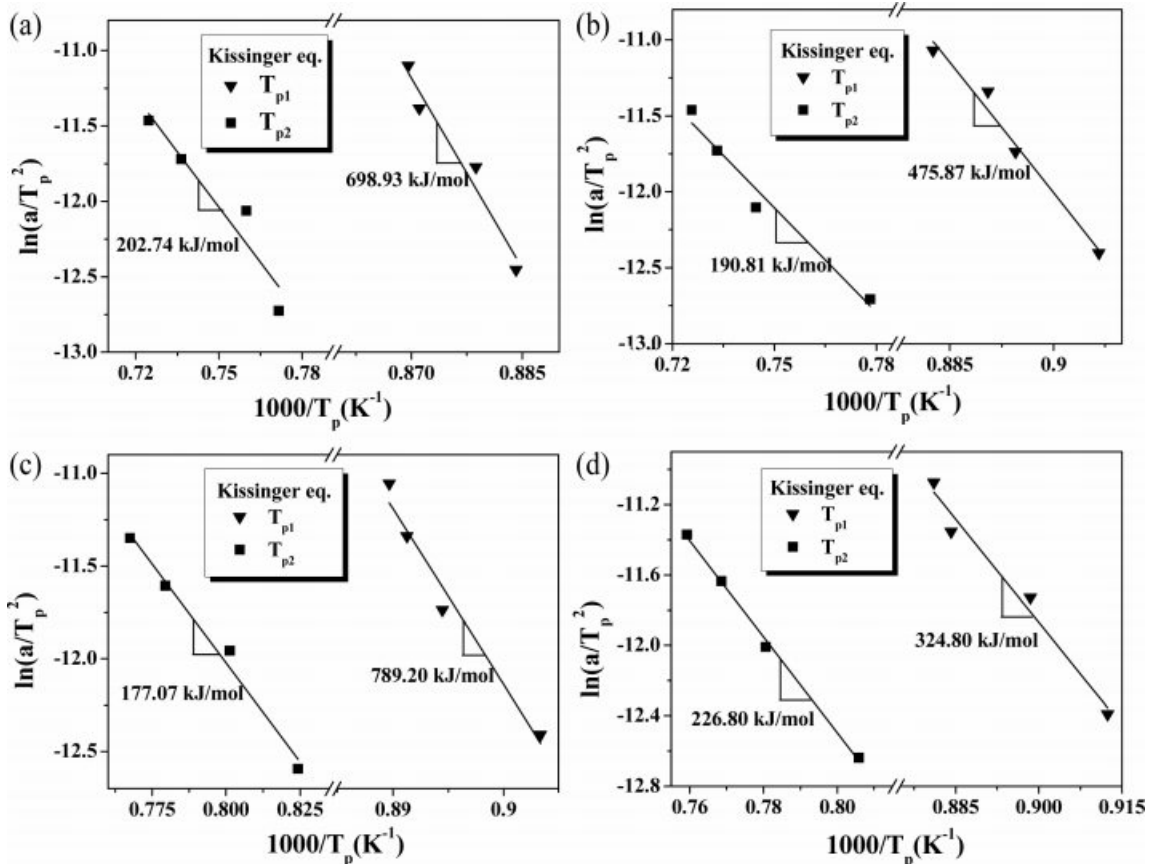


Fig. 2. The activation energy plots, derived by linear regression for crystallization of glaze (a) 0T, (b) 4T, (c) 8T, (d) 12T.

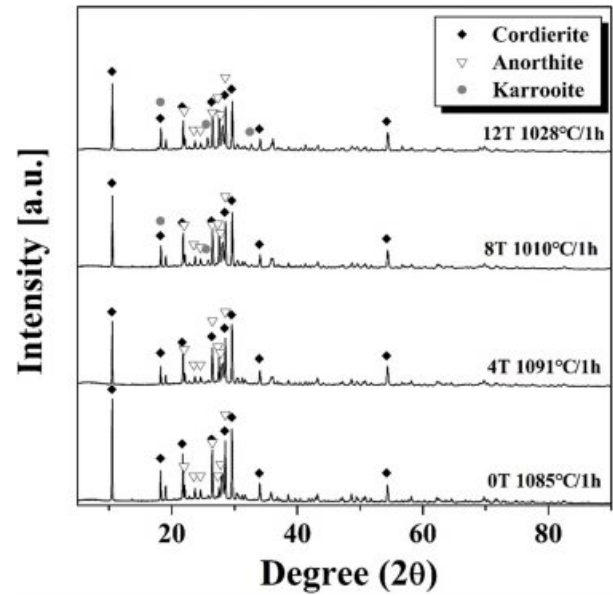
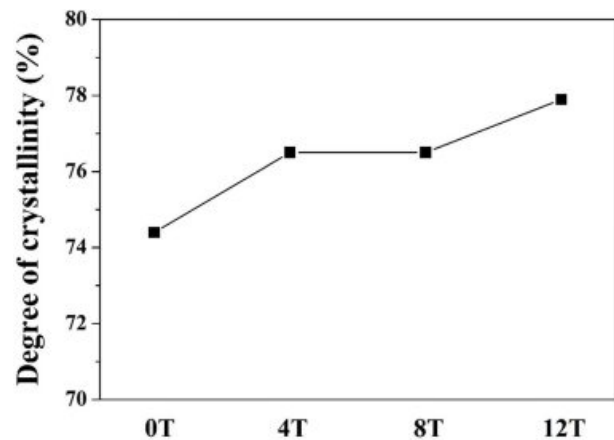
**Table 3.** The activation energy and Avrami constant of the glass-ceramic glaze.

Specimen I.D	$T_{p1}$		$T_{p2}$	
	Activation energy (kJ/mol)	Avrami constant	Activation energy (kJ/mol)	Avrami constant
0T	698.93	0.42	202.74	3.61
4T	475.87	0.61	190.81	3.53
8T	789.20	0.36	177.07	2.65
12T	324.80	0.62	226.80	2.92

2. Table 3 shows the Avrami constant ( $n$ ) calculated by Augis-Bennett's equation (2). The activation energy ( $E$ ) and Avrami constant ( $n$ ) values in the glass-ceramics are used to explain the crystallization mechanism. When the activation energy decreases from 400 kJ/mol to 200 kJ/mol, the crystallization mechanism changes from surface crystallization to bulk crystallization. In addition, it is known that surface crystallization when  $n = 1$  and  $n = 2-4$  indicates one to three-dimensional bulk crystallization [19, 20]. In the non-isothermal thermal analysis by using DTA, Avrami constant values of 0.36-0.62 were obtained with heat treatment at  $T_{p1}$  regardless of the composition, and it is difficult to form crystals in the glaze due to the Avrami constant lower than 1. In the case of heat treatment at  $T_{p2}$ , Avrami constants of 2.65 to 3.61 were obtained at 0T to 12T. The Avrami constant above 2.5 at  $T_{p2}$  is expected to induce bulk crystallization of the glaze. In all compositions, the activation energy ( $E$ ) of the glaze was 324-789 kJ/mol and 177-226 kJ/mol at  $T_{p1}$  and  $T_{p2}$ , respectively. Due to the low activation energy during heat treatment at  $T_{p2}$ , it is believed that the crystallization of the glaze will proceed by the bulk crystallization mechanism. According to the results of E. Ercenk et al., it is known that the bulk crystallization mechanism can yield glass-ceramic glass with high hardness due to high nucleation and crystal growth [21]. Therefore, in order to prepare a crystallization glaze based on the above results, heating was carried out for 1 h at a temperature of  $T_{p2}$  for each composition.

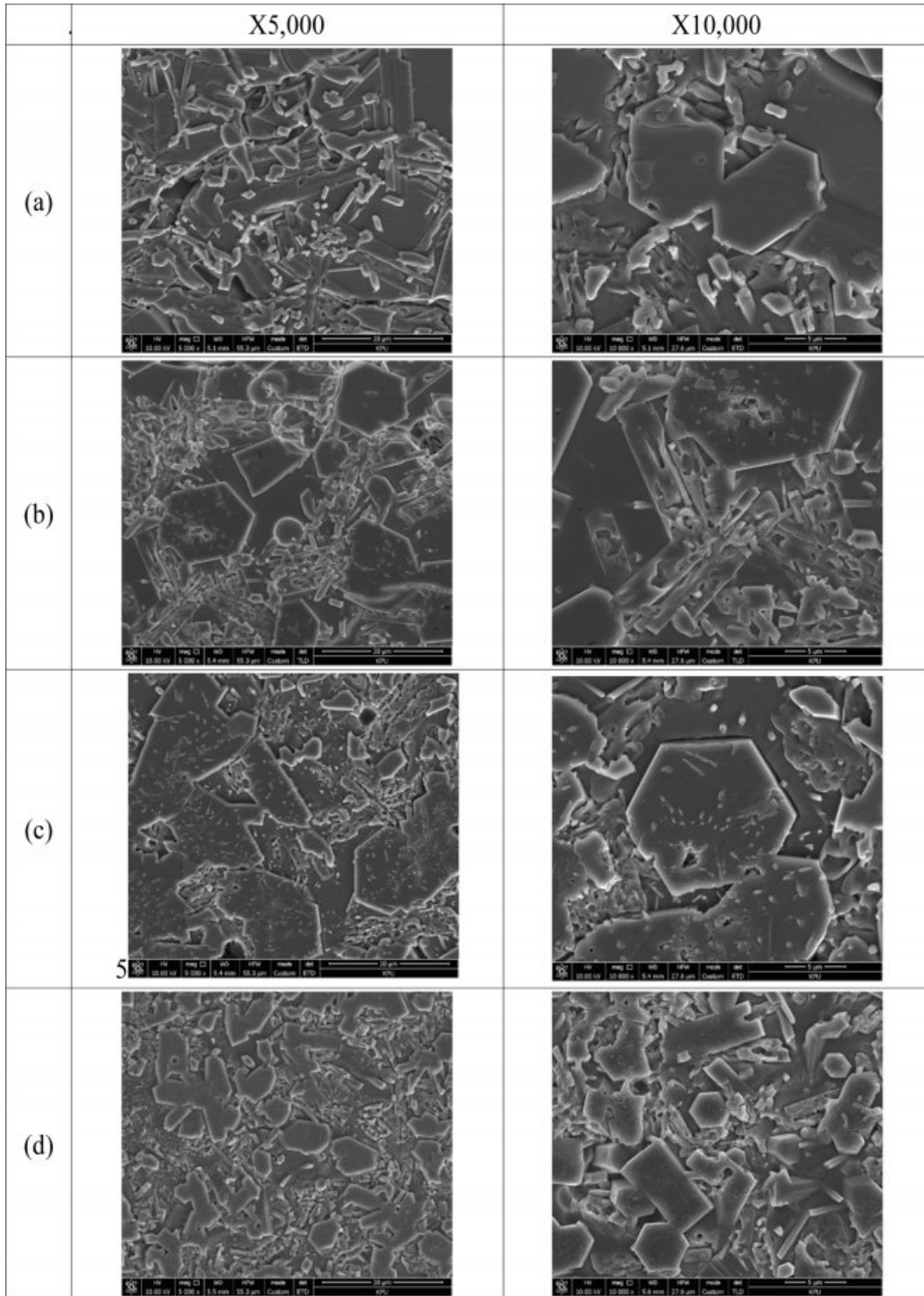
Fig. 3 presents the XRD analysis results of the glass-ceramic glaze heated for 1 h at the temperature of  $T_{p2}$ . Cordierite ( $Mg_2Al_4Si_5O_{18}$ ) and anorthite ( $CaAl_2Si_2O_8$ ) were observed in all compositions. In particular, karrooite ( $MgTi_2O_5$ ) crystal phases were observed at 8T and 12T with increased  $TiO_2$  content. The radii of  $Mg^{2+}$ ,  $Ti^{3+}$ , and  $Ti^{4+}$  ions forming the six coordinations are 0.0720, 0.0670, and 0.0605 nm, respectively, and  $Mg^{2+}$ ,  $Ti^{3+}$ , and  $Ti^{4+}$  ions are known to readily form an octahedral coordination when combined with  $O^{2-}$  [22]. Therefore, it is determined that the karrooite crystal phase was formed as the amount of  $TiO_2$  added was increased.

Fig. 4 shows the degree of crystallinity of the glaze, obtained by XRD analysis after heat treatment in  $T_{p2}$ . The degree of crystallinity values were 74.4% at 0T,

**Fig. 3.** The XRD analysis results of the glass-ceramic glaze heated for 1 h at the temperature of  $T_{p2}$ .**Fig. 4.** The degree of crystallinity of glass-ceramic glaze heated for 1 h at the temperature of  $T_{p2}$ .

76.5% at 4T, 76.5% at 8T, and 77.9% at 12T, respectively. The increase in the degree of crystallinity of the glaze with the addition of  $TiO_2$  is due to the nucleation and growth of karrooite crystalline phases including Ti in addition to the cordierite and anorthite crystalline phases.

Fig. 5 shows the microstructure of the glass-ceramic glaze heated for 1 h at the temperature of  $T_{p2}$ . In all compositions, plate-like angular and rod crystal phases were observed, and their size ranged from several  $\mu m$  to several tens  $\mu m$ . When the amount of  $TiO_2$  added was increased to 0-8 wt%, the size of the plate-shaped angular type showed a tendency to increase. However, when the amount of added  $TiO_2$  was 12 wt%, the crystal phase size was reduced. The crystalline phase observed in the SEM was analyzed by EDS for qualitative and quantitative analyses and the results are shown in Fig.



**Fig. 5.** The microstructure of the glass-ceramic glaze heated for 1 h at the temperature of  $T_{p2}$  (a) 0T, (b) 4T, (c) 8T, (d) 12T.

6. As a result of the EDS analysis of the square area of the SEM image, (a) showed 44.0 wt% of O, 23.4 wt% of Si, 16.0 wt% of Al, and 11.74 wt% of Ca. 46.4 wt%, Si was 23.2 wt%, Al was 13.5 wt%, and Mg was 8.8 wt%. Therefore, the rod crystal phase of (a) is determined to be anorthite ( $\text{CaAl}_2\text{Si}_2\text{O}_8$ ), and the angular crystal phase of (b) is cordierite ( $\text{Mg}_2\text{Al}_4\text{Si}_5\text{O}_{18}$ ).

Fig. 7 provides the results from measuring the density

and water absorption of the glass-ceramic glaze heated for 1 h at the temperature of  $T_{p2}$ . As the  $\text{TiO}_2$  content was increased, the density increased slightly from 2.56 to 2.65  $\text{g/cm}^3$  and the water absorption decreased from 0.6% at 0T, and below 0.1% at 4T. This correlates with the degree of crystallinity of the glaze shown in Fig. 4. The increased density and decreased water absorption of the glass-ceramic glaze is due to the structure of the

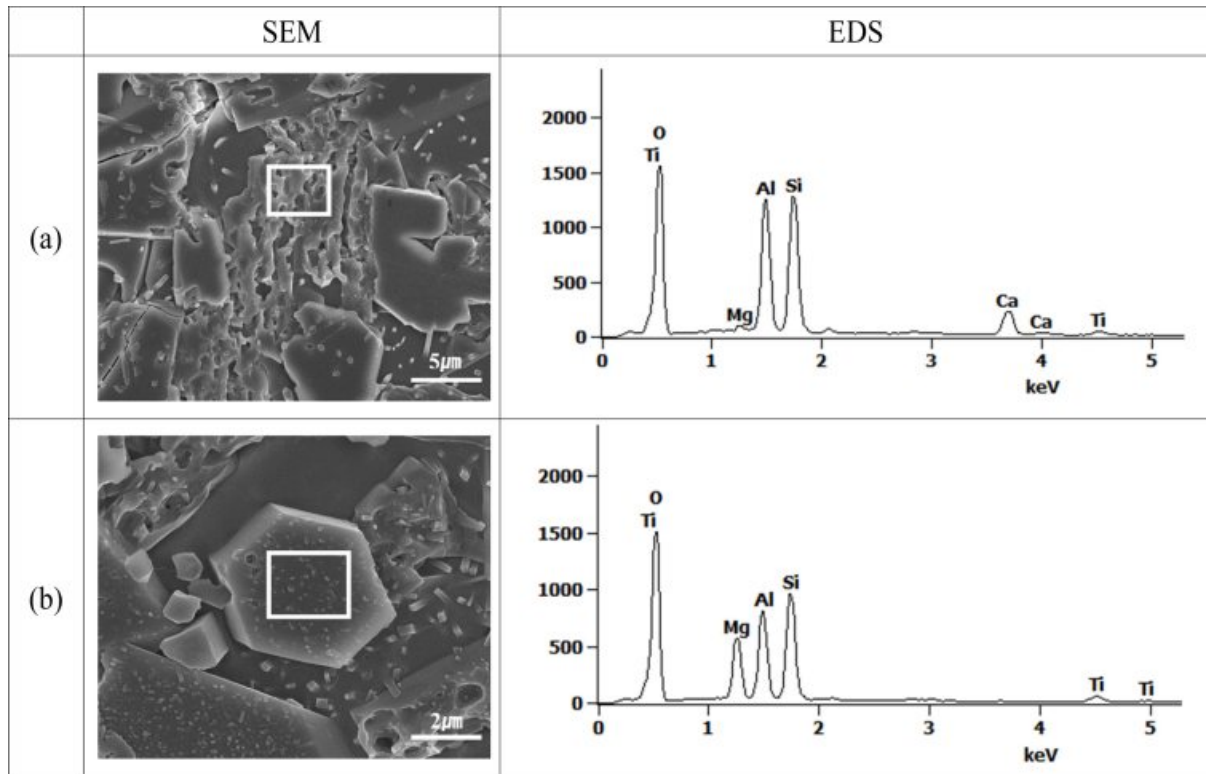


Fig. 6. The EDS of the glass-ceramic glaze (a) 8T, (b) 12T.

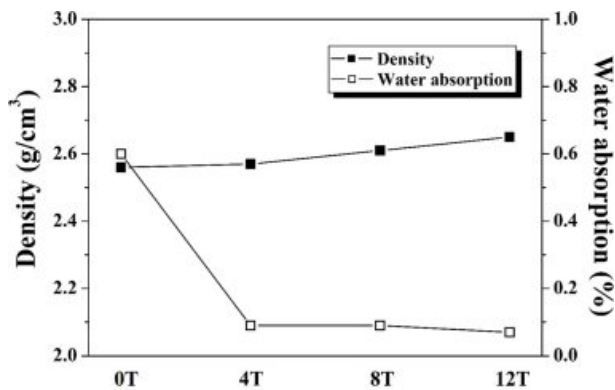


Fig. 7. The density and water absorption of the glass-ceramic glaze heated for 1 h at the temperature of  $T_{p2}$ .

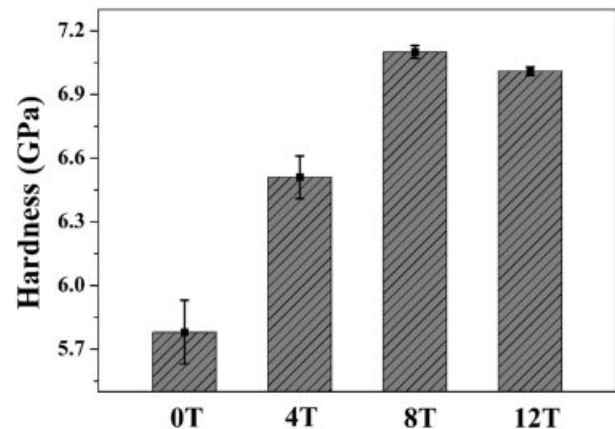


Fig. 8. A Vickers hardness graph of the glass-ceramic glaze heated for 1 h at a temperature of  $T_{p2}$ .

glaze becoming dense due to the ordered rearrangement of atoms as the degree of crystallinity of the amorphous glaze having a disordered structure increases. The degree of crystallinity has a significant influence on the hardness, density, transparency, and diffusion. However, the properties are not determined solely by the degree of crystallinity, but also by the size of the structural units or the molecular orientation [23]. The glass-ceramic glaze also satisfies the water absorption criterion (less than 3% ) of KS L 1001 ‘ceramic tiles’. [24].

Fig. 8 shows a Vickers hardness graph of the glass-ceramic glaze heated for 1 h at a temperature of  $T_{p2}$ . At 0T without  $\text{TiO}_2$ , the hardness was 5.78 GPa and at 8T with 8wt%  $\text{TiO}_2$ , the hardness increased to 7.10 GPa,

increasing by 22%. As the  $\text{TiO}_2$  content was increased from 0 wt% to 8 wt%, the hardness increased due to the increase in the degree of crystallinity and density of the glass-ceramic glaze. However, when the  $\text{TiO}_2$  content was 12 wt%, the hardness decreased slightly, which may be related to the crystal phase size in the microstructure. The microstructure in Fig. 5 showed that the cordierite and anorthite crystalline phases were the largest at 8T and tended to become smaller at 12T. Therefore, the size of the crystalline phase and the amount of crystalline phase (degree of crystallinity) are factors that affect the hardness of the glaze.

## Conclusion

In this paper, B<sub>2</sub>O<sub>3</sub> and CaCO<sub>3</sub> were added as flux and TiO<sub>2</sub> as a nucleating agent to a MgO-Al<sub>2</sub>O<sub>3</sub>-SiO<sub>2</sub> system to prepare a hardened cordierite based glass-ceramic. From the results of the DTA analysis, the lowest crystallization peaks of 849 °C (T<sub>p1</sub>) and 1,010 °C (T<sub>p2</sub>) were observed in 8T with the addition of 8wt% TiO<sub>2</sub>. Furthermore, from the results of the non-isothermal thermal analysis using DTA, it can be expected that the crystallization behavior of the glaze proceeds to bulk crystallization with an Avrami constant (n) of 2.65 to 3.61 when heat treated with T<sub>p2</sub>. The XRD analysis results revealed cordierite (Mg<sub>2</sub>Al<sub>4</sub>Si<sub>5</sub>O<sub>18</sub>) and anorthite (CaAl<sub>2</sub>Si<sub>2</sub>O<sub>8</sub>) crystalline phases in all compositions, and it was confirmed that karrooite (MgTi<sub>2</sub>O<sub>5</sub>) crystalline phases were additionally formed at 8T and 12T with high TiO<sub>2</sub> content. As the amount of TiO<sub>2</sub> added increased, the degree of crystallinity was high, and reached 76.5% at 8T. Microscopic observation using SEM showed that the size of the cordierite and anorthite crystal phase increased when the TiO<sub>2</sub> content was increased up to 0-8wt% and decreased at 12T. As the amount of TiO<sub>2</sub> added increased, the density of the glass-ceramic glaze increased and the water absorption tended to decrease. The hardness of the glass-ceramic glaze is determined by various factors such as the size of the crystalline phase, the degree of crystallinity, and microstructure, and the Vickers hardness value shows the highest 7.10 GPa hardness at 8T.

## Acknowledgments

This work was supported from the R&D program (KPP17002, Development of Functional Ceramic Tile using Surface Glaze Modification) by Korea Institute of Ceramic Engineering Technology.

## References

1. Y. Yu, H. Su, C. Peng, and J. Wu, *J. Eur. Ceram. Soc.* 39[2-3] (2019) 652-659.
2. S. Ghosh, K. S. Pal, N. Dandapat, J. Ghosh, and S. Datta, *J. Eur. Ceram. Soc.* 33[5] (2013) 935-942.
3. J. J. Reinoso, F. Rubio-Marcos, E. Solera, M. A. Bengochea, and J. F. Fernández, *Ceram. Int.* 36[6] (2010) 1845-1850.
4. H. Lua, M. Hea, Y. Liua, J. Guoa, L. Zhanga, D. Chena, H. Wanga, H. Xua, and R. Zhanga, *J. Ceram. Process. Res.* 12[5] (2011) 588-591.
5. G. Kaya, B. Karasu, and A. Cakir, *J. Ceram. Process. Res.* 12[2] (2011) 135-139.
6. V. Fuertes, M. J. Cabrera, J. Seores, D. Muñoz, J. F. Fernández, E. Enriquez, *Mater. Des.* 168 (2019) 1-10.
7. N. Obradović, N. Đorđević, S. Filipović, N. Nikolić, D. Kosanović, M. Mitrić, S. Marković, and V. Pavlović, *Powder Technol.* 218 (2012) 157-161.
8. G. H. Beall and L. R. Pinckney, *J. Am. Ceram. Soc.* 82[1] (1999) 5-16.
9. K. Pekkan and B. Karasu, *J. Eur. Ceram. Soc.* 29[9] (2009) 1571-1578.
10. R. Casasola, J. M. Rincón, and M. Romero, *J. Mater. Sci.* 47[2] (2012) 553-582.
11. O. A. Al-Harbi and E. M. A. Hamzawy, *Ceram. Int.* 40[4] (2014) 5283-5288.
12. S. A. M. Abdel-Hameed and I. M. Bakr, *J. Eur. Ceram. Soc.* 27[2-3] (2007) 1893-1897.
13. X. Hao, X. Hu, Z. Luo, T. Liu, Z. Li, T. Wu, A. Lu, and Y. Tang, *Ceram. Int.* 41[10] (2015) 14130-14136.
14. F. J. Torres and J. Alarcón, *J. Eur. Ceram. Soc.* 23[6] (2003) 817-826.
15. S. Ghosh, K. S. Pal, A. K. Mandal, N. Biswas, M. Bhattacharya, and P. Bandyopadhyay, *Mater. Charact.* 95 (2014) 192-200.
16. H. Savabieh, P. Alizadeh, B. Nayebi, and F. J. Clemens, *Ceram. Int.* 45[7] (2019) 8856-8865.
17. H. H. Jin, D. H. Kim, T. W. Kim, H. C. Park, and S. Y. Yoon, *Korean J. Mater. Res.* 21[6] (2011) 347-351.
18. Y. Sayuki, in "Glasses : For the People Who Want to make Glass for the First Time, translated to Korean" (Chungmungak Press, 2000) p.115-117.
19. H. S. Kim, I. O. Kim, M. H. Han, S. J. Kim, C. H. Suh, and K. H. Chang, *J. Korean Ceram. Soc.* 29[1] (1993) 14-19.
20. L. Deng, X. Zhang, M. Zhang, X. Jia, Z. Zhang, and B. Li, *J. Alloys Compd.* 785 (2019) 932-943.
21. E. Ercenk, B. Guven, and S. Yilmaz, *J. Non-Cryst. Solids.* 498 (2018) 262-271.
22. Y. J. Wang, S. M. Wen, Q. C. Feng, J. Liu, and W. C. Ren, *Trans. Nonferrous Met. Soc. China.* 26[9] (2016) 2518-2522.
23. B. E. Yekta, P. Alizadeh, and L. Rezazadeh, *J. Eur. Ceram. Soc.* 26[16] (2006) 3809-3812.
24. Korean Standards, No. KS L 1001 (2019) p.1-34.